CAP. 2. TRABAJO 11. T. 1

Est. CONGRESOS

DETECTION OF OVERPRESSURE ZONES BY USING SEISMIC DATA: THEORETICAL ASPECTS

José M. Carcione*, Anthony F. Gangi† and Hans B. Helle+

* Osservatorio Geofisico Sperimentale, P.O. Box 2011 Opicina, 34016 Trieste, ITALY.
Fax: +39 040 327521, e-mail: jcarcione@ogs.trieste.it

† Department of Geology and Geophysics, Texas A&M University, College Station, Texas 77843-3114, USA. Fax: +1 409 8456780, e-mail: gangi@tamu.edu

+ Norsk Hydro a.s., E & P Research Centre, N-5020 Bergen, NORWAY.
Fax: +47-55-996970. e-mail: hans.b.helle@nho.hydro.com

Resumen

La determinación de la presión poral con datos sísmicos es útil para planificar la perforación en función de presiones anómalas potencialmente peligrosas. Existen varias causas que generan una presión de fluido anómala en el subsuelo. Las dos causas más comúnes son la compactación desequilibrada y el *cracking*, o sea, la conversión de petróleo en gas.

Consideramos un modelo de deposición simple con sedimentación constante en el tiempo y gradiente geotérmico independiente de la profundidad. La conversión de petróleo en gas comienza a una determinada profundidad en una unidad geológica sellada por fallas, cuya permeabilidad es suficientemente baja, de modo tal que el incremento de presión causado por la generación de gas excede en gran medida la difusión hacia el exterior. La fracción de petróleo transformada en gas se obtiene suponiendo una reacción cinética cuyo período de reacción satisface la ecuación de Arrhenius. Entonces, la presión poral en exceso (respecto a la hidroestática) más las saturaciones de petróleo y gas se obtienen balanceando las masas y las fracciones volumétricas en el espacio poral.

Por otro lado, la compactación desequilibrada ocurre cuando la sedimentación es tan rápida que los fluidos no pueden escapar de los poros. El modelo considera un sistema cerrado y los poros saturados con agua y material orgánico. Como en el caso anterior, el balance de masa y volumen permite calcular la presión de los fluidos en función del tiempo de deposición y la profundidad.

La presión poral y la presión de confinamiento determinan la presión efectiva, la cual, a su vez, determina los módulos de compresión y corte de la matriz rocosa no saturada. Las propiedades sísmicas se obtienen con una modificación de la teoría de Biot para medios porosos saturados.

El análisis revela que las velocidades sísmicas disminuyen significamente cuando una cantidad pequeña de petróleo se convierte en gas. Esto es suficiente para que la presión poral iguale la presión de confinamiento. Hay cambios perceptibles en las velocidades cuando la presión diferencial es de 14 MPa, a la cual se llega cuando el 0.8 % del petróleo se convierte en gas. En el caso de compactación desequilibrada, la velocidad de las ondas P dependen en buena medida de la compresibilidad de los fluidos que saturan los poros. De ello depende si hay subpresión o sobrepresión. Variaciones perceptibles se producen cuando la presión diferencial es de 20 MPa, y cambios importantes ocurren debajo de 15 MPa.

Abstract

Knowledge of pore pressure using seismic data helps in planning the drilling process to control potentially dangerous abnormal pressures. Various physical processes cause anomalous pressures on an underground fluid. The two most common causes are non-equilibrium or disequilibrium compaction and cracking, i.e., oil to gas conversion.

We assume a simple basin-evolution model with a constant sedimentation rate and a constant geothermal gradient. Oil/gas conversion starts at a given depth in a reservoir volume sealed with faults whose permeability is sufficiently low so that the increase in pressure due to gas generation greatly exceeds the dissipation of pressure by flow. Assuming a first-order kinetic reaction, with a reaction rate satisfying the Arrhenius equation, the oil/gas conversion fraction is calculated. Balancing mass and volume fractions in the pore space yields the excess pore pressure and the oil and gas saturations.

On the other hand, disequilibrium compaction occurs when the sedimentation rate is so rapid that the pore fluids do not have a chance to escape from the pore space. The model assumes a closed system and that the pore space is filled with water and organic material. Balancing mass and volume fractions yields the fluid pressure versus time of deposition and depth of burial. Thermal effects are taken into account.

The pore pressure, together with the confining pressure, determines the effective pressure which, in turn, determines the bulk moduli of the rock matrix. Then, the seismic properties are calculated using a modification of Biot's theory for fully saturated porous solids.

The large change in the velocity is mainly due to the fact that the dry-rock moduli are

functions of the effective pressure, with the largest changes occurring at low effective pressures. The wave velocities and quality factors decrease with decreasing differential pressure (or effective pressure).

The analysis shows that velocities decreases significantly when only a small amount oil is converted to gas. This is sufficient to make the pore pressure equal to the confining pressure. Perceptible changes in the velocities occur when the differential pressure is 14 MPa, where about 0.8 % of oil has been converted to gas. In the case of disequilibrium compaction, the fluid mixture filling the pore space has a major influence on P-wave velocities and may cause underpressure or overpressure depending on its compressibility. Perceptible changes in the velocities occur when the differential pressure is 20 MPa and become significant when the differential pressure decreases to about 15 MPa.

Introduction

In deeply buried oil reservoirs, oil-to-gas cracking may increase the pore pressure to reach or exceed the lithostatic pressure (Chaney, 1950; Barker, 1990; Luo and Vasseur, 1996). Oil can be generated from kerogen-rich source rocks and flow through a carrier bed to a sandstone reservoir rock. If the reservoir is sealed on all sides by an impermeable shale or limestone, then the condition of a *closed system* will be satisfied for gas generation. Due to the presence of semi-vertical fault planes and compartmentalization, this condition holds for most North Sea reservoirs. Berg and Gangi (1998) developed a simple model to calculate the excess pore pressure as a function of the fraction of kerogen converted to oil and the fraction of oil converted to gas. Here, we use an extended version of this model for computing the porosity variations and fluid saturations as a function of the excess pore pressure.

On the other hand, disequilibrium compaction or mechanical compaction disequilibrium is a consequence of a rapid deposition compared to the time required for expelling the fluids from the pore space by gravitational compaction. In this situation, the fluids carry part of the load that would be held by grain contacts and abnormal pore pressures develop in the pore space. A description of this mechanism is given by Rubey and Hubbert (1959) and mathematical treatments of the problem are provided, for instance, by Bredehoeft and Hanshaw (1968), Smith (1971) and Dutta (1983).

The approach presented here assumes that if the rock is a shale, its permeability is extremely low, and if the rock is a sandstone, there are impermeable sealing faults and surrounding layers so that the fluids can not escape from the pore space. Balancing mass and volume fractions in the pore space yields the pore pressure, the saturations and the porosity versus time and depth of burial. Thermal effects are also taken into account. The pore pressure, together with the confining pressure, determines the effective pressure which, in turn, determines the dry-rock bulk moduli.

The seismic properties are calculated using a modification of Biot's theory for fully saturated porous solids. The wave velocities of the dry rock, determined by laboratory measurements, give estimates of its pore compressibility and bulk moduli in the low-frequency (relaxed) regime. Since dissipation mechanisms are mainly caused by grain/fluid interactions, dry-rock velocities are frequency-independent. On the other hand, measurements of ultrasonic wet-rock velocities provide the high-frequency limit (unrelaxed) velocities, which can be used to estimate the amount of velocity dispersion between the seismic and ultrasonic ranges and, therefore, the amount of attenuation. Using this information, the phase velocities and attenuation factors are computed as a function of pore pressure and frequency.

Overpressure due to cracking

Let us assume a reservoir at depth z. The lithostatic pressure for an average sediment density of $\bar{\rho}$ is equal to $p_c = \bar{\rho} g z$, where g is the acceleration of gravity. On the other hand, the hydrostatic pore pressure is approximately $p_H = \rho_w g z$, where ρ_w is the density of water.

For a constant sediment burial rate, S, and a constant geothermal gradient, G, the temperature variation of a particular sediment volume is $T = T_0 + Gz$, $z = St$, with a surface temperature T_0 at time $t = 0$. Typical values of G range from 20 to 30 °C/km, while S may range between 0.05 and 0.5 km/m.y. (m.y. = million years).

The mass of convertible oil changes with time t at a rate proportional to the mass present. Assuming a first-order kinetic reaction (Luo and Vasseur, 1996; Berg and Gangi, 1998) and a reaction rate following the Arrhenius equation, it can be shown that the oil-to-gas conversion factor is given by

$$F(t) = 1 - \exp[-\Phi(t)], \tag{1}$$

where

$$\Phi[T(t)] = \frac{A}{H}\left[\frac{T\exp(-E/RT)}{2 + E/RT} - \frac{T_i\exp(-E/RT_i)}{2 + E/RT_i}\right], \tag{2}$$

$H = GS$, R is the gas constant, and T_i is the initial temperature. The activation energy and infinite-temperature rate used in this work are $E = 52$ kcal/mol and $A = 5.5 \times 10^{26}$ / m.y. (Luo and Vasseur, 1996; Berg and Gangi, 1998).

The excess pore pressure at depth z is $\Delta p = p - p_H$, where p_H is the hydrostatic pore pressure and p is the pore pressure when a fraction F of oil has been converted to gas ($F = 0$ and $p = p_i = p_H$ at time t_i).

In general, compressional and shear wave velocities depend on effective pressure $p_e = p_c - np$, where $n \leq 1$ is the effective stress coefficient. Note that the effective pressure equals the confining pressure at zero pore pressure. It is found that $n \approx 1$ for static measurements of the compressibilities (Zimmerman *et al.*, 1986), while n is approximately linearly dependent on the differential pressure $p_d = p_c - p$ in dynamic experiments (Gangi and Carlson, 1996; Prasad and Manghnani, 1997):

$$n = n_0 - n_1 p_d, \tag{3}$$

where n_0 and n_1 are constant coefficients.

We assume the following functional form for the pore compressibility c_p as a function of effective pressure p_e:

$$c_p = c_p^{\infty} + \beta \exp(-p_e/p^*), \tag{4}$$

that the medium is fully saturated with oil and that, before oil/gas conversion occurs, the initial pressure, p_i, is hydrostatic. Balancing mass and volume fractions in the pore space, yields the relation between the oil-to-gas conversion factor F and the pore pressure p:

$$F = \left[D \frac{\rho_{gi}}{\rho_g(p,T)} - \exp(-c_o \Delta p + \alpha_o \Delta T) \right]^{-1} \{ \exp[E(\Delta p) + \alpha_p \Delta T] - \exp(-c_o \Delta p + \alpha_o \Delta T) \} . \tag{5}$$

where

$$E(\Delta p) = -c_p^{\infty} \Delta p_e + \beta p^* [\exp(-p_e/p^*) - \exp(-p_{ei}/p^*)].$$

In these equations, $D = \rho_o/\rho_{gi}$, where ρ_o is the oil density and ρ_{gi} is the initial gas density, ρ_g is obtained from the van Der Waals equation, c_o is the oil compressibility, α_o is the thermal expansion of oil, ΔT is the temperature increase, and α_p is the thermal expansion of the pore space.

With a surface temperature of 25 °C, a temperature gradient $G = 25$ °C/km, a sedimentation rate $S = 0.08$ km/m.y. and a reservoir volume at $z_i = z_1 = 2$ km, we have $t_i = t_1 = 25$ m.y. and $T_1 = 75$ °C. After 75 m.y., the depth of burial is $z_2 = 8$ km, $t_2 = 100$ m.y. and $T_2 = 225$ °C. On the other hand, if $\bar{\rho} = 2.4$ g/cm^3, the confining pressure has increased from $p_{c1} = 47$ MPa to approximately $p_{c2} = 188$ MPa, and the initial pore pressure is $p_i \simeq 20$ MPa (assuming $\rho_w = 1$ g/cm^3). If no conversion takes place, the final pore pressure would be the hydrostatic pressure at 8 km, i.e., approximately 78 MPa.

The experimental data for oil-saturated sandstone are available in Winkler (1985)-his Figures 3 and 4, and Tables 4 and 7. It is important to understand how the data were measured. After a suitable pore vacuum was achieved, confining pressure was increased to 40 MPa. Dry wave velocities were then obtained at successive pressures as the confining pressure decreased to 10 MPa. While still in the pressure vessel, the sample was saturated with oil to a pore pressure of 5 MPa. Differential pressure p_c was the increased to 10, 20 and 40 MPa, corresponding to the values $(p_c, p) = (20,10)$, $(40,20)$ and $(60,20)$ (in MPa). Note that Winkler calls the differential pressure the effective stress. The experiments on dry samples correspond to zero pore pressure. Best-fit plots of the dry-rock compressibility and shear modulus vs. confining pressure are

$$K_{sm}^{-1}[\mathrm{GPa}^{-1}] = 0.064 + 0.122 \exp(-p_c[\mathrm{MPa}]/6.48),$$

and

$$\mu_{sm}[\mathrm{GPa}] = 13.7 - 8.5 \exp(-p_c[\mathrm{MPa}]/9.14),$$

and c_p in GPa^{-1} is given by equation (4), with $c_p^\infty = 0.155$, $\beta = 0.6$, $p^* = 6.48$. The pore compressibility c_p has been obtained from the dry-rock bulk modulus by assuming that the porosity is that at hydrostatic pore pressure [this approximation is supported by experimental data obtained by Domenico (1977) and Han *et al.* (1986)]. The best-fit plots for c_p and K_{sm}^{-1} are illustrated in **Figure 1**.

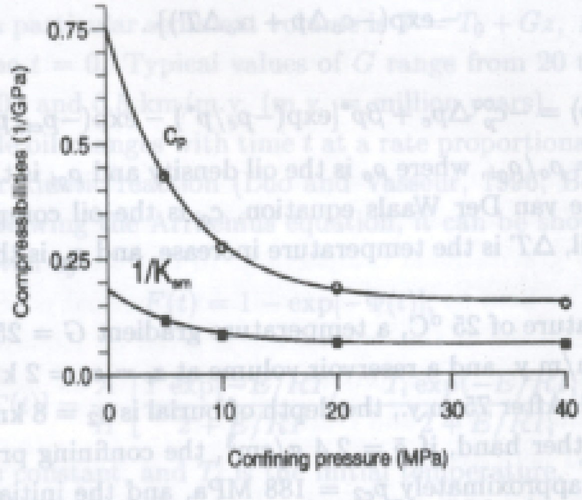

Figure 1

In order to obtain the moduli for different combinations of the confining and pore pressures we should make the substitution $p_c \rightarrow p_e = p_c - n(p_H + \Delta p)$, where we assume, following Gangi and Carlson (1996), that n depends on differential pressure as

$$n = n_0 - n_1 p_d, \quad n_0 = 1, \quad n_1 = 0.014 \text{ MPa}^{-1}.$$

This dependence of n versus differential pressure is in good agreement with the experimental values corresponding to the compressional velocity obtained by Christensen and Wang (1985) and Prasad and Manghnani (1997).

Table 1

GRAIN	$\rho_s = 2650$ kg/m^3
	$K_s = 37$ GPa
	$\mu_s = 39$ GPa
FLUIDS	$\rho_o = 890$ kg/m^3
	$K_o = 2.16$ GPa
	$\alpha_o = 5 \times 10^{-4}$ C^{-1}
	$\eta_o = 237$ cP
	$\eta_g = 0.017$ cP
	$\rho_w = 1040$ kg/m^3
	$K_w = 2.25$ GPa
	$\alpha_w = 5 \times 10^{-4}$ C^{-1}
	$\eta_w = 1.8$ cP
MATRIX	$K_{sm} = 15.45$ GPa
	$\mu_{sm} = 13.48$ GPa
	$\phi = 0.203$
	$\kappa = 10^{-12}$ m^2
	$\alpha_p = 2 \times 10^{-4}$ C^{-1}

1 cP = 0.001 Pa s

Table 1 indicates the properties for Berea sandstone and the different fluids, with the values corresponding to those at the initial (hydrostatic) pore pressure. The oil density and bulk modulus are assumed pressure-independent and equal to the values indicated by Winkler (1985) for 20 MPa. The oil and gas viscosities as a function of temperature and pore pressure are taken from Luo and Vasseur (1996).

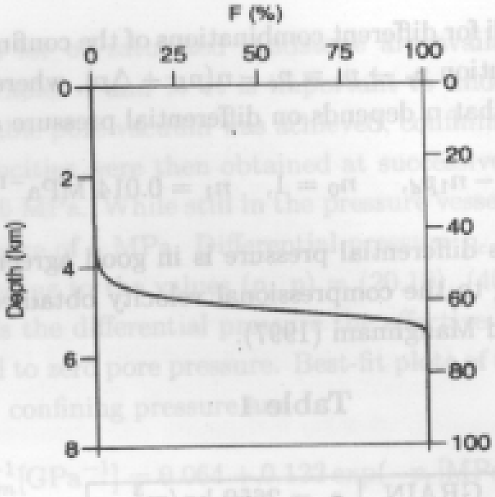

Figure 2

Figure 2 shows the oil/gas conversion factor [equation (1)] as a function of depth and time. The high activation energy requires either a long time or deep burial, on the order of 4.5 to 5 km, before appreciable fractions of conversion occur, but significant fractional conversions occur at 3 km. The pore-pressure buildup with depth is shown in **Figure 3**.

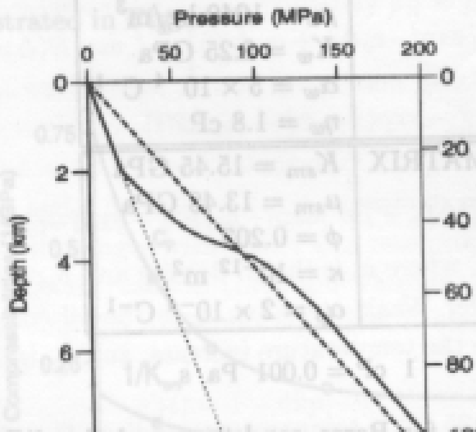

Figure 3

The pressure rapidly increases for very small fractions of oil converted to gas. This is due to the low compressibility of the rock. Beyond the lithostatic pressure the effective pressure becomes negative and the pore compressibility increases (see **Figure 1**), making the rock highly compliant. This precludes a rapid increase of the pore pressure, which follows the lithostatic pressure below 4 km depth.

Biot's theory successfully describes the wave propagation properties of synthetic porous media such as sintered glass beads. In natural porous media such as sandstone, discrepancies between Biot's theory and measurements are due to complex pore shapes that are not present in simple synthetic media (Gist, 1994). Skeleton-fluid mechanisms are modeled by generalizing the coupling modulus to a time dependent relaxation function, based on the generalized linear solid with L dissipation mechanisms (Carcione, 1998): The mixture organics/water behaves as a composite fluid with properties depending on the constants of the constituents and their relative concentrations. This problem has been analyzed by Berryman *el al.*, (1988).

The low-frequency wave velocities versus excess pore pressure and differential pressure for this model are shown in **Figure 4**.

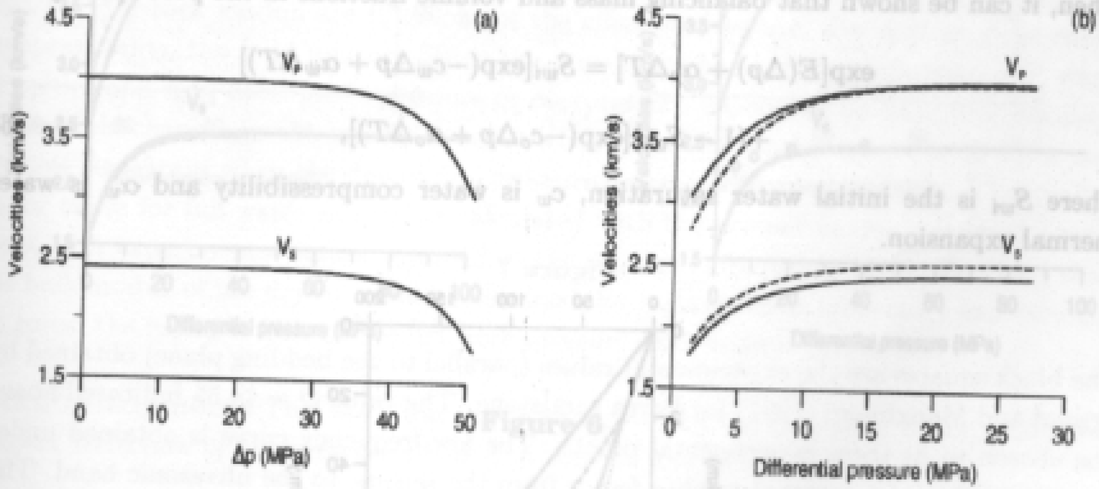

Figure 4

An excess pore pressure of 50 MPa corresponds to zero differential pressure. The oil/gas conversion starts at a differential pressure of 27.4 MPa, which corresponds to an onset time of approximately 25 million years, when the sandstone is fully saturated with oil. As can be appreciated, the velocities decrease substantially after an excess pore pressure of approximately 35 MPa. This is partially due to the replacement of oil by gas at high oil saturations, but mainly to the decrease in the matrix bulk moduli K_{sm} and μ_{sm} caused by the decrease in effective pressure.

Overpressure due to disequilibrium compaction

The case of non-equilibrium compaction is that in which the sedimentation rate is so rapid that the pore fluids do not have a chance to 'escape'. We assume that the pore space is filled with organic material and water, that the compressibilities of the organics and water are independent of pressure and temperature, and that of the rock is independent of temperature but depends on pressure. At time t_i, corresponding to depth z_i, the volume of rock behaves as a closed system. That is, if the unit is a shale, its permeability is extremely low, and if the unit is a sandstone, the permeability of the sealing faults is sufficiently low so that the rate of pressure increase greatly exceeds the dissipation of pressure by flow. Pore pressure excess is measured relative to hydrostatic pressure.
Then, it can be shown that balancing mass and volume fractions in the pore space yields

$$\exp[E(\Delta p) + \alpha_p \Delta T] = S_{wi}[\exp(-c_w \Delta p + \alpha_w \Delta T)] + (1 - S_{wi})[\exp(-c_o \Delta p + \alpha_o \Delta T)], \quad (6)$$

where S_{wi} is the initial water saturation, c_w is water compressibility and α_w is water thermal expansion.

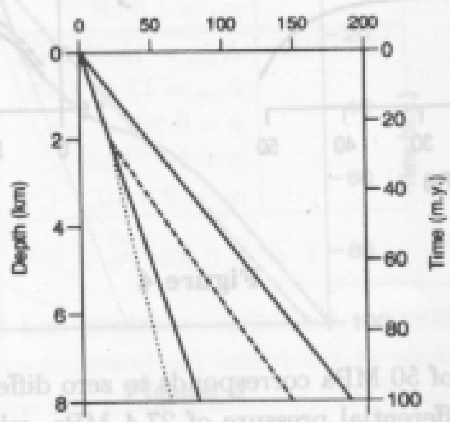

Figure 5

The solution of equation (6) gives the pore pressure p as a function of depth and deposition time, with $\Delta T = T - T_i = G(z - z_i) = GS(t - t_i)$ for a constant geothermal gradient and a constant sediment burial rate.

The experimental data for oil-saturated sandstone is that of Winkler (1985), illustrated in the previous example. Table 2 indicates the properties for water. The pore-pressure buildup with depth for $S_w = 0$ (dotted line) and $S_w = 1$ (broken line) is shown in Figure 5, where the continuous lines represent the hydrostatic and lithostatic pressure. As can be appreciated, the rock is underpressured for full oil saturation and increasing water saturation gives overpressure. For a given rock, the pore pressure depends on the compressibility of the mixture filling the pore space. For low compressibilities the pore pressure may exceed the lithostatic pressure.

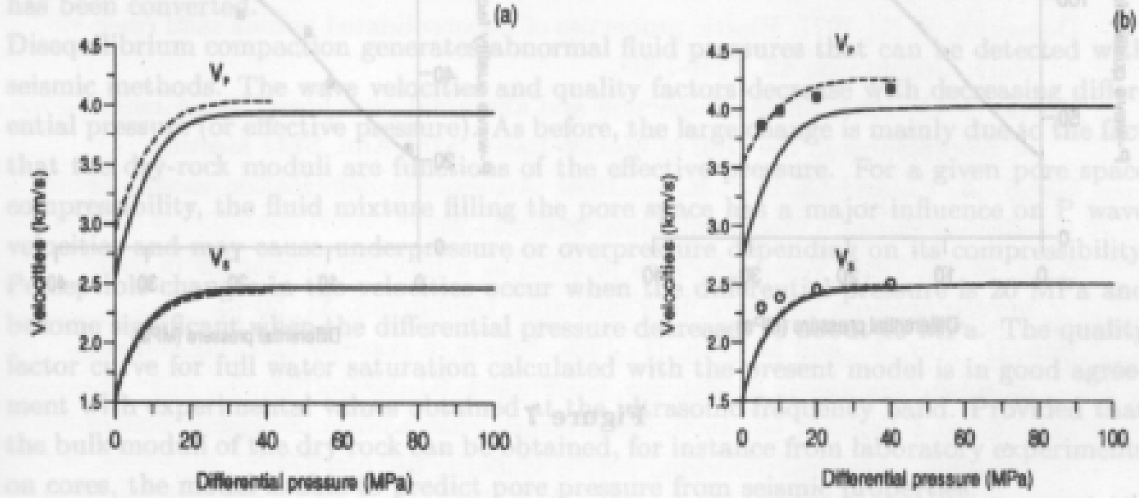

Figure 6

Figure 6 shows (a) the low-frequency (25 Hz) and (b) the ultrasonic (1 MHz) compressional and shear velocities versus differential pressure p_d for $S_w = 0$ (continuous line) and $S_w = 1$ (broken line). The black squares and empty circles are the experimental compressional and shear velocities obtained by Winkler (1985) for oil-saturated Berea sandstone. We use a continuous spectrum of dissipation mechanisms for Biot's coupling modulus, from 1 Hz to 1 MHz and a Q factor of 14.55, regardless of the saturations. The differential pressure is approximately 40 MPa at 8 km depth for the rock saturated with water, and nearly 126 MPa for the oil-saturated rock (see **Figure 5**). The pore-fluid affects mainly the compressional velocity, with unrelaxed velocities higher than relaxed velocities, as expected. The discrepancies between the experimental values and the continuous lines (full oil saturation) are due to the fact that Winkler's oil compressibility is closer to water compressibility than the one used in this work. Moreover, Winkler's data correspond to a frequency of 400 kHz.

The quality factors versus differential pressure for water-saturated Berea sandstone (S_{wi} = 1) are represented in **Figure 7**, where (a) is the low-frequency curve (25 Hz) and (b) is the ultrasonic curve (1 MHz).

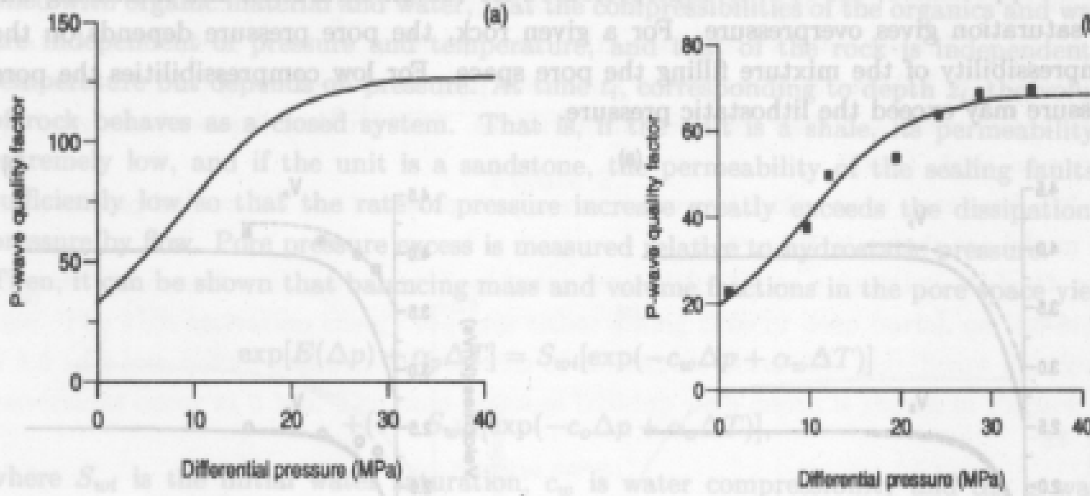

Figure 7

The black squares are the experimental values (parallel to the bedding plane) obtained by Prasad and Manghnani (1997) for Berea sandstone. The value Q = 14.55 indicated above was chosen to fit these experimental points. The low-frequency curve is obtained under the assumption of a constant quality factor from the seismic to the ultrasonic band. The behavior of this curve, as well as the ultrasonic one, indicates that overpressure implies low quality factors and therefore high wave attenuation.

Conclusions

The variations of P-wave and S-wave velocities have been determined as a function of excess pressure due to oil/gas conversion and disequilibrium compaction. In the first case, the results for a model in which a reservoir volume is buried at a constant sedimentation rate for a geothermal gradient, which is both constant in time and depth, show that the velocities decreases significantly when only a small amount (about 2.5 %) of the oil in the closed reservoir is converted to gas. This small conversion of oil to gas is sufficient to make the pore pressure equal to the confining pressure. This large change in the velocity is mainly due to the fact that the dry-rock moduli are functions of the effective pressure, with the largest changes occurring at low effective pressures. In fact, porosity changes and fluid moduli and density do not have a major effect on the velocities. The effective pressure decreases since the pore pressure increases due to the conversion of the high-density oil to the low-density gas. Perceptible changes in the velocities occur when the differential pressure is 14 MPa, where about 0.8 % of oil has been converted to gas, and become significant when the differential pressure decreases to 10 MPa, where about 1.1 % has been converted.

Disequilibrium compaction generates abnormal fluid pressures that can be detected with seismic methods. The wave velocities and quality factors decrease with decreasing differential pressure (or effective pressure). As before, the large change is mainly due to the fact that the dry-rock moduli are functions of the effective pressure. For a given pore space compressibility, the fluid mixture filling the pore space has a major influence on P wave velocities and may cause underpressure or overpressure depending on its compressibility. Perceptible changes in the velocities occur when the differential pressure is 20 MPa and become significant when the differential pressure decreases to about 15 MPa. The quality factor curve for full water saturation calculated with the present model is in good agreement with experimental values obtained at the ultrasonic frequency band. Provided that the bulk moduli of the dry rock can be obtained, for instance from laboratory experiments on cores, the model is able to predict pore pressure from seismic properties.

Acknowledgments This work was partly supported by the European Union under the project *Detection of overpressure zones with seismic and well data.*

References

Barker, C., 1990, Calculated volume and pressure changes during the thermal cracking of oil to gas in reservoirs, AAPG Bulletin, 74, 1254-1261.

Berryman, J. G., Thigpen, L., and Chin, R. C. Y., 1988, Bulk elastic wave propagation in partially saturated porous solids, J. Acous. Soc. Am., 84(1), 360-373.

Berg, R. R., and Gangi, A. F., 1998, Primary migration by oil-generation microfracturing in low-permeability source rocks: Application to the Austin chalk, Texas, submitted to AAPG Bulletin.

Bredehoeft, J. D., and Hanshaw, B. B., 1968, On the maintenance of anomalous fluid pressures: I. Thick sedimentary sequences, Geol. Soc. Am. Bull., **79**, 1097-1106.

Carcione, J. M., 1998, Seismic attributes of petroleum source rocks, submitted to Geophysics.

Chaney, P. E., 1950, Abnormal pressure and lost circulation, World Oil, **130**, 122-126.

Christensen, N. I., and Wang, H. F., 1985, The influence of pore pressure and confining pressure on dynamic elastic properties of Berea sandstone, Geophysics, **50**, 207-213.

Domenico, S. N., 1977, Elastic properties of unconsolidated porous sand reservoirs, Geophysics, **42**, 1339-1368.

Dutta, N. C., 1983, Shale compaction and abnormal pore pressures: A model of geopressures in the Gulf of Mexico Basin, 53rd Ann, SEG Meeting.

Gangi, A. F., and Carlson, R. L., 1996, An asperity-deformation model for effective pressure, Tectonophysics, **256**, 241-251.

King, M. S., 1966, Wave velocities in rocks as a function of changes in overburden pressure and pore fluid saturants, Geophysics, **31**, 50-73.

Han, D., Nur, A., and Morgan, D., 1986, Effects of porosity and clay content on wave velocities in sandstones, Geophysics, **51**, 2093-2107.

Luo, X., and Vasseur, G., 1996, Geopressuring mechanism of organic matter cracking: numerical modeling, AAPG Bulletin, **80**, 856-874.

Prasad, M., and Manghnani, M. H., 1997, Effects of pore and differential pressure on compressional wave velocity and quality factor in Berea and Michigan sandstones, Geophysics, **62**, 1163-1176.

Rubey, W. W., and Hubbert, M. K., 1959, Role of fluid pressure mechanics of overthrust faulting, II. Overthrust belt in geosynclinal area of Western Wyoming in light of fluid pressure hypothesis, Geol. Soc. Am., **70**, 167-205.

Smith, J. E., 1971, The dynamics of shale compaction and evolution of pore-fluid pressure, Math. Geol., **3**, 239-263.

Winkler, K. W., 1985, Dispersion analysis of velocity and attenuation in Berea sandstone, J. Geophys. Res., **90**, 6793-6800.

Zimmerman, R. W., Somerton, W. H., and King, M. S., 1986, Compressibility of porous rocks, J. Geophys. Res., **91**, 12765-12777.